(Received 31 December 2024, Accepted 27 February 2025, Scheduled 14 March 2025)

A Novel Method for Multi-Function Radar Work Mode Boundary Detection

Yuxin Fu, Jiantao Wang*, Jie Huang, Tongxin Dang, and Yiming Li

The National Digital Switching System Engineering and Technological Research and Development Center Zhengzhou 450000, China

ABSTRACT: Work mode boundary detection can provide basic information units for the recognition of consecutive work modes in the intercepted multi-function radar (MFR) pulse sequence. The existing boundary detection methods tend to detect false boundaries when the pulse parameters vary drastically within the work mode, such as when the pulse repetition interval (PRI) modulation type is stagger or agile. To address the issue of over-detection of the work mode transition boundary, a new work mode boundary detection method is proposed based on the arc crossings (AC). It utilizes AC to quantify and annotate the similarities within MFR work modes. Without relying on prior knowledge, it can accurately capture the structural characteristics of the boundary transition and effectively adapt to different pulse parameter modulation types. The experimental results show that it reduces the segmentation probabilistic error by 8.7% and false alarm rate by 19.85% compared to the baseline algorithm.

1. INTRODUCTION

Multi-function radar (MFR) can perform various tasks in different work modes and achieve multiple functions in sequence, such as search, target tracking, and missile guidance [1–3]. To realize different functions and perform particular tasks, MFR transmits many pulse sequence segments with a specific timing structure and agile waveforms in a certain order, which brings severe challenges to electronic reconnaissance missions [4]. Identifying the work mode of the target MFR is crucial for assessing the threat level and obtaining other essential information [5]. Accurate work mode boundary detection on the intercepted pulse sequence is the prerequisite for extracting the pulse sequence segments corresponding to each work mode and subsequent MFR work mode recognition.

Several scholars have conducted related research in recent years. The research based on supervised learning was first proposed in 2020 [6]. It utilized an improved long-short-time neural network to train pulse sequences. It had high accuracy and low miss rate but required a priori information, such as train data labeled with work mode. However, labeling intercepted radar pulse sequences in electronic reconnaissance is usually difficult. Therefore, it is necessary to develop blind processing methods based on unsupervised learning. The latest research proposed a work mode boundary detection method based on the recurrence plot without relying on prior information in 2022 [7]. It extracted the main features through singular value decomposition and finally realized boundary detection using distance similarity measurements. It addressed the problem of severe degradation of algorithmic performance without prior knowledge, but it had the new problem of high false alarm rates due to over-reliance on the texture features of the recurrence plot.

The MFR work mode boundary detection is a segmentation problem that can be solved using segmentation techniques in nature [8]. In previous research, the fast low-cost semantic segmentation (FLOSS) algorithm is designed to solve similar problems in the area of healthcare [9]. It exploits the similarity of local patterns within the time series, such as ECG signals, by taking the local minimum value of the corrected arc crossings (CAC) as the segmentation basis. However, unlike continuous ECG signals, the modulation type of the pulse in the intercepted pulse sequence changes drastically at the work mode transition boundary and remains stable within the work mode [10]. There are consecutive local minimum values of the CAC caused by sub-sequences containing different work modes segments when dealing with the intercepted pulse sequence. Thus, the FLOSS easily extracts the wrong boundaries in advance.

Therefore, we require an improvement of the FLOSS algorithm to adapt to the MFR signal features. Suppose there is a sub-sequence of the MFR signal in which pulses are all within the same work mode. It will find its nearest neighbor within the current work mode until its ending pulse slides to the next work mode, forming a smooth region with the low height of AC. The height of the AC should be high when the work mode transition boundary is within the sub-sequence. We introduce local standard deviation to convert smooth regions into troughs and remove the correction step. By setting the appropriate threshold to search the troughs, this letter avoids over-detection problems at the non-inflection points, especially when the pulse parameters change dramatically under the stagger or agile modulation type.

The main contributions of our work are summarized as follows:

* Corresponding author: Jiantao Wang (18538324298@126.com).

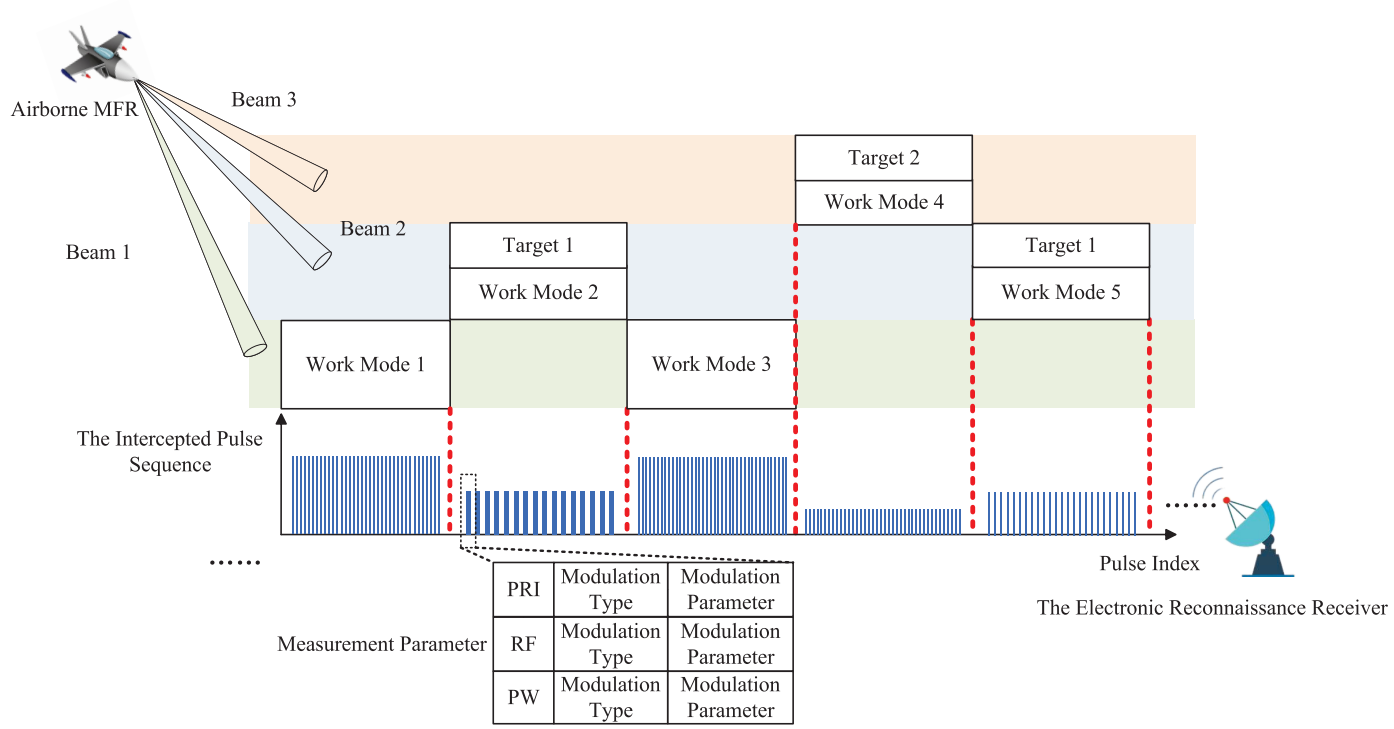

FIGURE 1. Illustration of the intercepted radar pulse sequence X. The airborne MFR emits pulses continuously in different beam directions to perform different tasks. The pulse stream is intercepted by the electronic reconnaissance receiver and called the intercepted pulse sequence X. Each segment in X corresponds to a work mode. Each pulse is represented by the measurement parameter.

1) Pioneering application of arc crossings (AC) for radar signal processing: We propose the first use of AC for radar work mode boundary detection. By quantifying the spatial density of nearest-neighbor arcs, AC can capture the structural stability within a work mode and the abrupt transitions at boundaries, effectively overcoming the sensitivity of traditional recurrence plot texture features to local parameter fluctuations.

2) Enhanced FLOSS algorithm with local standard deviation and smooth region search: We introduce local standard deviation and smooth region search strategies to improve the FLOSS algorithm. This enhancement effectively mitigates spurious boundary interference caused by drastic pulse parameter variations, such as those in stagger or agile modulation types. Provided that the measurement error remains below 25%, the algorithm ensures that at least 95.75% of input pulses are correctly assigned to their corresponding work mode segments, with a maximum of one spurious boundary detected. Compared to the latest work mode boundary detection algorithm and baseline algorithm, it reduces the false alarm rate by 27.83% and 19.85% respectively.

The rest is summarized as follows. Section 2 gives the boundary detection problem formulation. Section 3 describes the principles and flow of the boundary detection algorithm. Section 4 obtains the parameter configurations and simulation results. Section 5 summarizes the research.

2. BOUNDARY DETECTION PROBLEM FORMULATION

Assume that the MFR is a system in two or more discrete inherent states [11]. We can monitor it with special sensors, such as the electronic reconnaissance receiver. For the receiver, the intercepted pulse sequence after signal deinterleaving and the radar type identification can be formally denoted as follows:

$$X = \{\vec{x_1}, \vec{x_2}, \ldots, \vec{x_T}\} \in R^{m \times T} \tag{1}$$

where $\vec{x_t} = (x_{1t}, x_{2t}, \ldots, x_{mt})^{\mathrm{T}}, (t = 1, 2, \ldots, T)$ is an m-dimensional pulse at pulse index t. The m-dimensional parameters of the intercepted pulse generally refer to its measurement parameter of the receiver, including PRI, radio frequency (RF), and pulse width (PW) [12]. The discrete inherent states are generally equivalent to the work modes defined in this paper, which are modulation combinations on the three selected pulse parameters. The modulation types typically include constant, agile, stagger, sliding, and jittered [13]. We would expect X from the receiver to reflect the current work mode of the MFR, as shown in Figure 1. Given an intercepted pulse sequence X with $K + 1 (K \geq 1)$ work mode segments, each segment contains $N_i, (i = 1, 2, \ldots, K + 1)$ pulses. Thus, the task of work mode boundary detection can be regarded as inferring K boundaries between changes in the modulation combinations. We can obtain the corresponding set of pulse indexes $S = t_1, t_2, \ldots, t_K \subset 1, 2, \ldots, T$ and the set of work mode labels $L = \underbrace{l_1, l_1, \ldots, l_1}_{N_1}, \underbrace{l_2, l_2, \ldots, l_2}_{N_2}, \ldots, \underbrace{l_{K+1}, l_{K+1}, \ldots, l_{K+1}}_{N_{K+1}}$.

3. BOUNDARY DETECTION ALGORITHM BASED ON AC

We utilize the shape characteristics of AC to design a novel boundary detection algorithm. The overall boundary detection

algorithm flowchart is shown in Figure 1. The steps of the proposed algorithm are as follows.

3.1. Matrix Profile Index Calculation

Given an 3-dimensional pulse sequence $P = \{\vec{p_1}, \vec{p_2}, \ldots, \vec{p_T}\} \in R^{3\times T}$. Select the sub-sequence $P_{i\ldots i+W} = \{\vec{p_i}, \vec{p_{i+1}}, \ldots, \vec{p_{i+W-1}}\} \in R^{3\times W}, i = 1, 2, \ldots, T-W+1$ from P. To quantify the similarities between various sub-sequences segments within P, the Euclidean distance matrix D is denoted as follows:

$$D_{i,j} = \|P_{i\ldots i+W-1} - P_{j\ldots j+W-1}\|_2 \quad (2)$$

For each sub-sequence, the location of its nearest neighbor can be stored in an ordered vector, and we call the vector the matrix profile index (MPI). MPI is a vector of integers and denoted as follows:

$$I_i = j, if D_{i,j} = \min(D_{i,1}, D_{i,2}, \ldots, D_{i,T-W+1}) \quad (3)$$

By storing the neighboring information this way, we can efficiently retrieve the nearest neighbor of $P_{i\ldots i+W}$ by accessing the i-th element in the MPI.

3.2. AC Generation

We can visualize $P_{i\ldots i+W}$ and its nearest neighbor $P_{j\ldots j+W}$ as an arc drawn from location i to j. The AC summarizes the spatial layout of the arcs along with the number of "arc" crossing over each sub-sequence index i. AC is a time series of non-negative integer values, and the i-th index in the AC specifics how many nearest neighbor arcs from the MPI spatially cross over sub-sequence index i. The AC of the i-th sub-sequence is defined as:

$$AC_i = \sum_{k=1}^{T-W+1} \mathbb{I}\left(i \in [k, k+W-1] \cap [I_k, I_k+W-1]\right) \quad (4)$$

where $\mathbb{I}(\cdot)$ is the indicator function, which equals 1 if the sub-sequence i lies within the overlapping interval of sub-sequence k and its nearest neighbor sub-sequence I_k, and 0 otherwise.

3.3. Smooth Region Search

In AC, the number of "arcs" crossing decreases significantly when the internal pulse of the sub-sequence is at the transition boundary. It forms smooth regions of the troughs of AC, and each smooth region's beginning position corresponds to the transition boundary between different work modes. Therefore, the boundary detection task can be transferred to search for the smooth region of the AC. To quantify the degree of dispersion of AC, we use the normalized standard deviation (NSD) within the sliding window of length W (equal to the size of the sub-sequence). Let $\sigma_i = \left(\frac{\sum_{k=i}^{i+W-1}(AC_i - \overline{AC})}{W-1}\right)^{\frac{1}{2}}$ denotes the standard deviation of AC within a sliding window of length W. The NSD is calculated as:

$$NSD_i = \frac{\sigma_i - \min(\sigma)}{\max(\sigma) - \min(\sigma)} \quad (5)$$

where $\sigma = \{\sigma_1, \sigma_2, \ldots, \sigma_{T-W+1}\}$ represents the set of standard deviations across all sliding windows. Then, search for the local minimum of NSD with an interval of W. When NSD_i is less than the set $Threshold (0 \le Threshold \le 1)$, the boundary search result $T = \{t_i\} \in R^{1\times K}$ is denoted as $t_i = i + W$. To summarize, the flowchart of the work mode boundary detection algorithm is shown in Figure 2. The overall procedure of the proposed algorithm is presented in Algorithm 1.

Algorithm 1 Algorithm of the work mode boundary detection.

Input: Intercepted pulse sequence $X \in \mathbb{R}^{m\times T}$, sub-sequence length W, and smoth region detection threshold $Threshold$

Output: Boundary positions $S = \{t_1, t_2, \ldots, t_K\}$

Stage 1: Compute matrix profile index (MPI)
for each $i \in [1, T-W+1]$ **do**
  Extract sub-sequence $P_{i\ldots i+W-1}$
  for each $j \in [1, T-W+1]$ **do**
    Calculate pairwise Euclidean distances $D_{i,j} = \|P_{i\ldots i+W-1} - P_{j\ldots j+W-1}\|_2)$
  end for
  Store nearest neighbor index $I_i = \arg\min_j D_{i,j}$
end for
Stage 2: Generate arc crossings (AC)
for each $i \in [1, T]$ **do**
  Initialize $AC_i = 0$
  for each $k \in [1, T-W+1]$ **do**
    if $i \in [k, k+W-1] \cap [I_k, I_k+W-1]$ **then**
      $AC_i \leftarrow AC_i + 1$
    end if
  end for
end for
Stage 3: Compute normalized standard deviation (NSD) and detect boundaries via thresholding
for each $i \in [1, T-W+1]$ **do**
  Compute $NSD_i = \frac{\sigma_i - \min(\sigma)}{\max(\sigma) - \min(\sigma)}$
  Initialize $S = \emptyset$ and $t_K = -\infty$
  if $NSD_i < Threshold$ and $i > t_K + W$ **then**
    Add $t = i + W$ to S
    Update $t_K = i$
  end if
end for
return Outputs

4. SIMULATION RESULTS AND ANALYSIS

4.1. Dataset Configuration

As shown in Table 1, this section executes simulation experiments utilizing an open MFR signal dataset to verify the performance of the proposed boundary detection algorithm. It was created by Chi et al. [7] and contained five work modes. Each work mode is uniquely defined by the modulation type combinations of PRI, RF, and PW. For example, mode 1 uses fixed PRI, staggered RF, and agile PW modulation, while mode 2 employs sliding PRI, fixed RF, and fixed PW. Notably, the value of the pulse parameter under the fixed modulation type remains constant over time. The value of the pulse parameter under the remaining four modulation types shows dynamic temporal variations consistent with the modulation characteristics detailed in

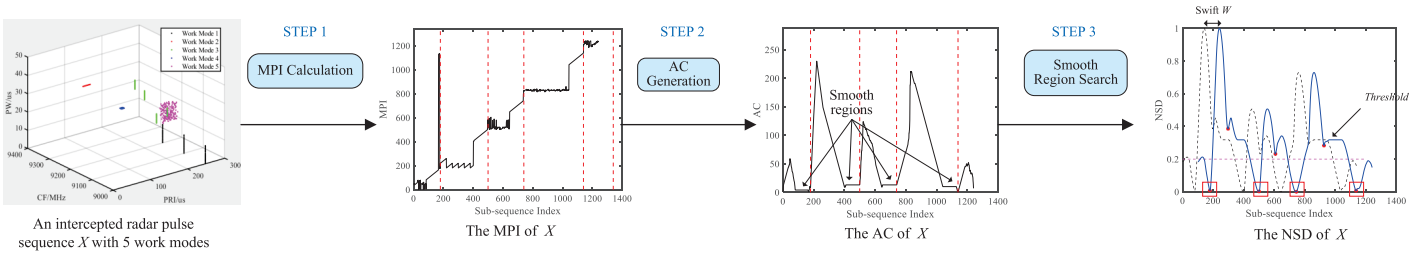

FIGURE 2. Flowchart of the work mode boundary detection algorithm.

TABLE 1. The definition of five work modes for MFR.

Work mode	PRI/us [100, 300]	RF/MHz [9000, 9500]	PW/us [1, 50]	Pulse number
1	Fixed	Stagger	Agile	180
2	Sliding	Fixed	Fixed	320
3	Stagger	Stagger	Agile	240
4	Jittered	Jittered	Fixed	400
5	Agile	Agile	Agile	200

Table 2. The modulation parameters for each modulation are drawn uniformly from the ranges provided in [13]. All the simulation experiments are carried out in MATLAB 2021 and are run on 2.00GHz (CPU) and 32.00 GB memory (RAM).

4.2. Algorithm Assumption

The proposed algorithm requires the following conditions to ensure optimal performance. First, the input signal must contain at least two segments of different work modes to ensure that the algorithm has sufficient pulse samples for feature extraction. Considering the varying pulse counts across different radar work modes in practical scenarios, the interception duration of the receiver antenna beam aligned with the target MFR should be adjusted based on operational requirements. Second, the parameter measurement error must not exceed 25%. Within this tolerance range, the algorithm ensures that at least 95.75% of input pulses are correctly assigned to their corresponding work mode segments, with a maximum of one spurious boundary detected. Moreover, the decrease of signal-to-noise ratio (SNR) increases the measurement error in parameters such as PRI, RF, and PW. The algorithm's tolerance for the measurement error inherently constrains the minimum acceptable SNR of the received signals.

4.3. Evaluation Metrics

We use two main criteria to assess the performance of boundary detection results. The evaluation metrics are computed on the proposed dataset basis and averaged over 500 Monte Carlo simulations. One is the probabilistic error P_d [14] between actual segmentation T_r and algorithmic segmentation results S for work mode. P_d is denoted as follows:

$$P_d = \frac{1}{T} \cdot \sum_{i=1}^{T-d-1} |\delta_{T_r}(i, i+d+1) - \delta_S(i, i+d+1)| \quad (6)$$

where T is the length of the sequence to be segmented, and d is half of the average of the lengths of the sequences resulting from the segmentation of the algorithm. If the i-th pulse and $i+d+1$-th pulse are in the same segment, $\delta(i, i+d+1) = 1$; otherwise, $\delta(i, i+d+1) = 0$. The smaller the P_d is, the more accurate the boundary detection is.

The other is the estimation rate (ER) [14] of the segmentation result. ER is denoted as follows:

$$ER = \frac{K^*}{K} \quad (7)$$

where K is the number of actual work mode boundaries, and K^* is the obtained segmentation. $ER > 1$ means that the algorithm has a high false alarm rate because the number of boundaries obtained by the algorithm segmentation is more than the number of actual work mode boundaries. The algorithm has a high false alarm rate. Similarly, $ER < 1$ means that the algorithm has a high missed alarm rate. $ER = 1$ means the algorithm has the highest accuracy.

4.4. Analysis on Setting Parameters of the Proposed Method

As mentioned above, we introduce the sub-sequence length W and $Threshold$ of normalized standard deviation to solve the work mode boundary problem. Now we investigate the influence of these two setting parameters on the segmentation accuracy of the proposed method. In this experiment, 6000 pulse segments corresponding to each work modes are generated without adding noise. Then randomly and uniformly select 6 pulse segments with different work modes to form one intercepted radar pulse sequence. In total, there are 1000 intercepted radar pulse sequences to be detected. To evaluate the impact of sub-sequence length and threshold, we conducted experiments with varying values of $W = 50, 100, 150, 200, 250$ and $Threshold = 0.05, 0.1, 0.15, 0.2, 0.25$. Then the P_d and ER for different settings of the length of sub-sequence W and the P_d of normalized standard deviation are shown in Figure 3.

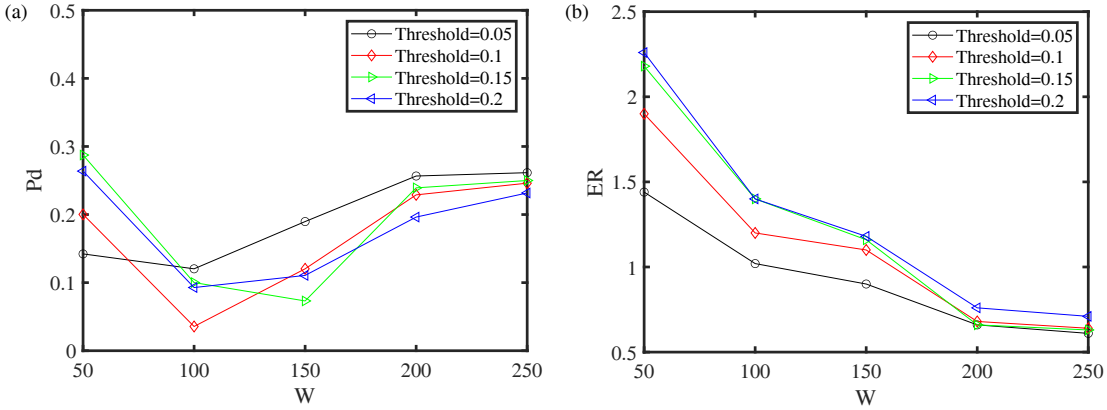

FIGURE 3. The curves of (a) P_d and (b) ER variation with W for different $Threshold$.

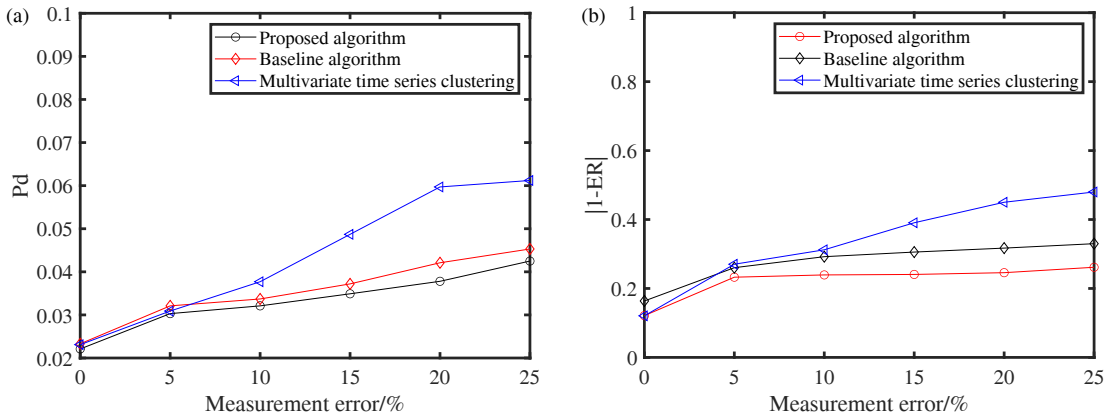

FIGURE 4. The performance comparison results of (a) P_d and (b) $|1 - ER|$.

The results indicate that if we want to reduce the miss rate of the algorithm, we can set the small input parameter values. This is because when $W = 50$, $Threshold = 0.2$, the ER is the highest, which means that if W is shorter and $Threshold$ higher, the structure characteristics shown in AC will be more obvious. Therefore, the algorithm will be more sensitive to boundary pulses. But to improve detection accuracy, we must set appropriate input parameters. This is because when $W = 100$, $Threshold = 0.1$, $P_d = 0.0356$ is lowest, which means that if W and $Threshold$ are too short, the structure characteristics of work mode internal inter-pulse modulations will be mistaken for the structure characteristics of work mode transition boundaries. Therefore, in the practical application, we can select appropriate input parameters according to the current extraction effect and the change of assessment criteria.

4.5. Comparative Experiment

To verify the effectiveness of the proposed method, we compare it with the baseline algorithm and the multivariate time series clustering method developed by research [2]. The multivariate time series clustering method is an unsupervised learning approach designed for processing pulse sequences from non-cooperative MFR and demonstrates robust recognition performance in the cited research. The radar pulse samples are generated according to Table 1 and Table 2. The Gaussian noise is added to the samples to quantify the measurement error, which causes pulse parameters jitter in the range of 0% to 25% of the central value according to the Gaussian distribution. The results of experiments described by P_d and ER are shown in Figure 4 when $W = 100$, Threshold = 0.1, and $K = 5$. From the performance change curves, we can see that the proposed method demonstrates the best overall performance when the measurement error rises from 0% to 25%, achieving 19.45%, 8.70% reduction in average P_d and 27.83%, 19.85% reduction in average ER compared to the clustering method and baseline algo-

TABLE 2. The modulation type and characteristic of pulse parameter.

Pulse parameter	Type	Characteristic
PRI	Sliding	Periods = 8 ∼ 40
	Stagger	Periods = 3 ∼ 5
	Jittered	Range = 5 ∼ 10%
	Agile	Range = 100 ∼ 300us
RF	Stagger	Periods = 3 ∼ 6
	Jittered	Range = 5 ∼ 10%
	Agile	Range = 100 ∼ 300us
PW	Agile	Range = 1 ∼ 50us%

rithm respectively. The higher accuracy and robustness advantage of our algorithm over the other two methods is because the calculation of AC is based on the relative position relationship of sub-sequences instead of absolute parameter values, which is naturally robust to the measurement error. In contrast, the baseline algorithm suffered from over-detection in extracting the transition boundaries of the work modes with stagger and agile inter-pulse modulation. The clustering method assumes that different work modes are distinctly separated in the feature space. However, when sub-sequences near work mode transition boundaries are affected by Gaussian noise, they tend to form continuous transitional regions within the feature space, leading to blurred cluster boundaries.

5. CONCLUSION

This research investigates a novel method for detecting the transition boundary of MFR work mode based on the characteristics of the intercepted pulse sequence, which can effectively alleviate the "over-detection" problem when detecting the work mode with stagger modulation type. The boundary detection problem is first formulated using the pulse segment parameter model. Then, an improved sequence segmentation algorithm is designed by utilizing the similarity of the pulse inside the work mode and the difference of the boundary pulse. Simulation results demonstrate that it reduces the segmentation probabilistic error by 8.7% and the false alarm rate by 19.85% compared to the baseline algorithm.

REFERENCES

[1] Weber, M. E., J. Y. N. Cho, and H. G. Thomas, "Command and control for multifunction phased array radar," *IEEE Transactions on Geoscience and Remote Sensing*, Vol. 55, No. 10, 5899–5912, 2017.

[2] Fan, R., M. Zhu, and X. Zhang, "Multivariate time series feature extraction and clustering framework for multi-function radar work mode recognition," *Electronics*, Vol. 13, No. 8, 1412, 2024.

[3] Li, B., Z. Zhou, and L. Sun, "Ultra-wideband planar dipole array antenna for multifunction phased array radars," *Progress In Electromagnetics Research Letters*, Vol. 90, 135–142, 2020.

[4] Liu, Z.-M., "Recognition of multifunction radars via hierarchically mining and exploiting pulse group patterns," *IEEE Transactions on Aerospace and Electronic Systems*, Vol. 56, No. 6, 4659–4672, 2020.

[5] Zhu, M., Y. Li, and S. Wang, "Model-based time series clustering and interpulse modulation parameter estimation of multifunction radar pulse sequences," *IEEE Transactions on Aerospace and Electronic Systems*, Vol. 57, No. 6, 3673–3690, 2021.

[6] Li, Y., M. Zhu, Y. Ma, and J. Yang, "Work modes recognition and boundary identification of MFR pulse sequences with a hierarchical seq2seq LSTM," *IET Radar, Sonar & Navigation*, Vol. 14, No. 9, 1343–1353, 2020.

[7] Chi, K., J. Shen, Y. Li, L. Wang, and S. Wang, "A novel segmentation approach for work mode boundary detection in MFR pulse sequence," *Digital Signal Processing*, Vol. 126, 103462, 2022.

[8] Wang, K., J. Lu, A. Liu, and G. Zhang, "TS-DM: A time segmentation-based data stream learning method for concept drift adaptation," *IEEE Transactions on Cybernetics*, Vol. 54, No. 10, 6000–6011, 2024.

[9] Yeh, C.-C. M., Y. Zhu, L. Ulanova, N. Begum, Y. Ding, H. A. Dau, D. F. Silva, A. Mueen, and E. Keogh, "Matrix profile I: All pairs similarity joins for time series: A unifying view that includes motifs, discords and shapelets," in *2016 IEEE 16th International Conference on Data Mining (ICDM)*, 1317–1322, Barcelona, Spain, Dec. 2016.

[10] Zhao, Y., X. Wang, and Z. Huang, "Multi-function radar modeling: A review," *IEEE Sensors Journal*, Vol. 24, No. 20, 31 658–31 680, 2024.

[11] Xu, Z., Q. Zhou, Z. Li, J. Qian, Y. Ding, Q. Chen, and Q. Xu, "Adaptive multi-function radar temporal behavior analysis," *Remote Sensing*, Vol. 16, No. 22, 4131, 2024.

[12] Zhai, Q., Y. Li, Z. Zhang, Y. Li, and S. Wang, "Few-shot recognition of multifunction radar modes via refined prototypical random walk network," *IEEE Transactions on Aerospace and Electronic Systems*, Vol. 59, No. 3, 2376–2387, 2022.

[13] Kauppi, J.-P., K. Martikainen, and U. Ruotsalainen, "Hierarchical classification of dynamically varying radar pulse repetition interval modulation patterns," *Neural Networks*, Vol. 23, No. 10, 1226–1237, 2010.

[14] Gharghabi, S., Y. Ding, C.-C. M. Yeh, K. Kamgar, L. Ulanova, and E. Keogh, "Matrix profile VIII: Domain agnostic online semantic segmentation at superhuman performance levels," in *2017 IEEE International Conference on Data Mining (ICDM)*, 117–126, New Orleans, LA, USA, Nov. 2017.